

Medium effects on the quarkonia states above critical temperature

Arpit Parmar,^{1,*} Bhavin Patel,^{2,†} and P C Vinodkumar^{1,‡}

¹*Department of Physics, Sardar Patel University, Vallabh Vidyanagar-388 120, India.*

²*Department of Physical Sciences, P D Patel Institute of Applied Sciences, Changa, India*

(Dated: November 27, 2024)

We present the quarkonia correlators for charmonium and bottomonium systems in the pseudoscalar, vector and scalar channels. For the description of quark-antiquark interaction we adopt the temperature dependant colour screening potential of the power law form. The spectroscopic parameters defined from the model are employed in the spectral functions to compute the quarkonia correlators. We find considerable medium modifications to the effective masses of the quarkonia as well as in the behaviour of the respective radial wave functions. These modifications are then reflected in the computed correlators. The general behaviour of correlators in the vector and scalar channel are in accordance with the latest lattice results while their behaviour in the pseudoscalar channels are found to be different.

I. INTRODUCTION

The behaviour of heavy quarkonium states (charmonium and bottomonium) in a hot and dense medium have attracted considerable experimental and theoretical interest. Heavy quarkonia play an important role in studying hot and dense strongly interacting matter. Study of the properties of heavy quarkonia above deconfinement temperature is of extreme interest for current Relativistic heavy ion collider (RHIC) experiments [1, 2]. The topics of interest in these studies include survival probabilities as bound state at some temperature in quark gluon plasma and in medium transport properties of heavy and light quarks. Because of larger quark mass the heavy quarkonia can survive and remain in bound state above the deconfinement temperature T_c . The binding energy analysis has become important for such studies based on either potential models [3] or by Lattice methods [4–6]. The lattice results of quarkonia correlator studies predicts existence of $1S$ charmonium states upto $1.6T_c$ and of $1P$ states (χ_{c0} and χ_{c1}) states upto $1.1T_c$. The present results on bottomonium study predicts existence of $1S$ states (η_b and Υ) upto temperatures $2.3T_c$ and for $1P$ states (χ_b) upto $1.15T_c$. Which are in contradiction with the earlier potential model calculations which predict dissolution of charmonium states below $1.1T_c$ [7, 8]. With the large number of excited charmonia and bottomonia states known our earlier understanding based on potential models have been reviewed recently [3] and systematic variations in the confinement strength has been introduced to explain the observed quarkonia spectra. Such a modification to the string tension of the confining part of the potential then be understood in terms of the medium effects. Based on such an attempt, here we extend our earlier works on the spectroscopy and decay properties of quarkonia using coulomb plus power law potential (CPP_ν) model to a systematic study based on the

quarkonia correlators for charm and bottom quark systems. To incorporate the medium effects on the binding energy of quarkonia we generalize the usual coulomb plus power law (CPP_ν) form of the potential with a medium dependant exponential screening factor which reduces to the coulomb plus power law form in the absence of the medium effect. In section II we discuss the method to compute spectral functions and correlators. The spin average mass and the wave function dependant decay constants are derived in section III. Finally, we discuss and summarize our results for quarkonia correlators against different choices of power exponent ν in section V.

II. EUCLIDEAN CORRELATORS AND SPECTRAL FUNCTIONS

The temperature dependence of the meson correlators can provide information about the fate of quarkonia states above deconfinement. The imaginary time Euclidean correlation functions of meson currents $G(\tau, T)$ are reliably calculated on the lattice

$$G(\tau, T) = \int d\omega \sigma(\omega, T) K(\tau, \omega, T) \quad (1)$$

Where, $\sigma(\omega, T)$ is the zero temperature spectral function and $K(\tau, \omega, T)$ is the kernel of integration and can be written as,

$$K(\tau, \omega, t) = \frac{\cosh(\omega(\tau - \frac{1}{2T}))}{\sinh(\frac{\omega}{2T})} \quad (2)$$

In lattice QCD calculation the spectral function $\sigma(\omega)$ can be extracted out from the information of correlators using the maximum entropy method [9]. While, the potential models employ the spectral function to extract out the quarkonia correlators. Following ref [10] the spectral function can be written as,

$$\sigma(\omega) = \sum_i 2M_i F_i^2 \delta(\omega^2 - M_i^2) + \frac{3}{8\pi^2} \omega^2 \theta(\omega^2 - s_0) f(\omega, s_0) \quad (3)$$

* arpitspu@yahoo.co.in

† azadpatel2003@yahoo.co.in

‡ pothodivinod@yahoo.com

The first term arises from the pole contributions from the bound states, and the second term is the perturbative continuum above some threshold s_0 . Here, we consider the form of $f(\omega, s_0)$ motivated by leading order perturbative calculations with massive quarks as [3],

$$f(\omega, s_0) = \left(a_H + b_H \frac{s_0^2}{\omega^2} \right) \sqrt{1 - \frac{s_0^2}{\omega^2}} \quad (4)$$

The calculated coefficients of a_H and b_H at leading order by [11] are shown in Table I. The value of threshold energy s_0 is somewhat arbitrary for single flavour heavy quark only. Here, s_0 is chosen such that no resonance above it is possible. The remaining parameters M_i and wave function dependant decay constants F_i are deduced from the potential model adopted for the present study. To see the temperature effect on the spectral function and to compare with the lattice QCD results one usually computes the ratio of this correlators to the reconstructed one $G(\tau, T)/G_{recon}(\tau, T)$, where $G_{recon}(\tau, T)$ is given by,

$$G_{recon}(\tau, T) = \int_0^\infty d\omega \sigma(\omega, T=0) K(\tau, \omega, T) \quad (5)$$

Here, $G_{recon}(\tau, T)$ corresponds to the spectral function at the zero temperature. The temperature dependance in the $G_{recon}(\tau, T)$ comes only from the kernel of the integration.

TABLE I. The coefficients (a_H, b_H) in different mesonic channel [11]

System	a_H	b_H
scalar	-1	1
pseudoscalar	1	0
vector	2	1
axial-vector	-2	3

III. EXTRACTION OF SPIN AVERAGE MASS (M_i) AND DECAY CONSTANTS (F_i)

The spin average mass and decay constants appeared in the expression of the spectral function (Eqn. 3) are deduced using an appropriate model description of the hadronic state. Here, for the description of the quarkonia states we consider temperature dependant screened potential of the form,

$$V(r, T) = -\frac{\alpha}{r} e^{-\mu(T)r} + \frac{\sigma}{A\mu(T)} (1 - e^{-A\mu(T)r^\nu}) \quad (6)$$

Here, α and σ are the coupling constant and string tension respectively. The exponent, ν is the variation that we have introduced here to account for the non-linear dependance on the interquark distance of the potential. Different choices of the exponent, ν describes

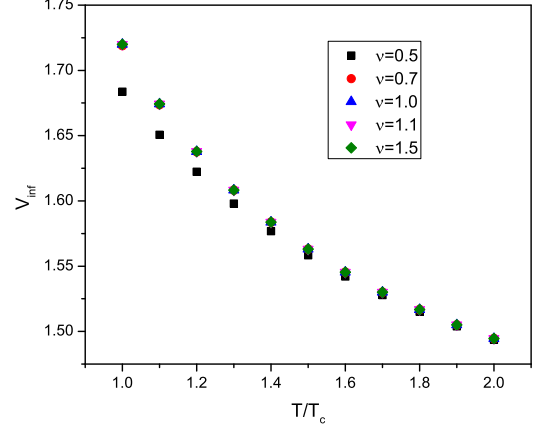


FIG. 1. $V(r = \infty, T)$ for different temperature at different potential exponent

different strength of the interquark interaction. The screening mass parameter $\mu(T)$ is taken as, $\mu(T) = 0.24 + 0.31(T/T_c - 1) \text{ GeV}$ [3] with critical temperature $T_c = 0.270 \text{ GeV}$. Here, we have chosen $A = 1 \text{ GeV}^{\nu-1}$. Here, the screening potential attains finite value at infinite separation i.e. $V(r = \infty, T)$. Hence, each quark has an additional thermal energy of $V_\infty/2$ in the bound state. The minimum energy above which the quark-antiquark pair can freely propagate is $2m + V_\infty$. Hence, the minimum energy threshold can be defined in this case as $s_0 = 2m + V_\infty$. The potential V_∞ for different temperature is shown in Fig. 1 for different potential exponent. Similarly, the pole mass m_i corresponds to $m_i = m + V_\infty/2$ against T/T_c for different potential exponent ν are shown in Fig. 2 for bottomonium and charmonium states. V_∞ found to be decreasing with increase in temperature above T_c . Similar observation is observed on lattice calculations while calculating quark and gluon propagators in coulomb gauge [12]. In the absence of the medium effect (at zero temperature) the potential in Eqn. 6 reduces to the form

$$V(r) = -\frac{\alpha}{r} + \sigma r^\nu \quad (7)$$

The parameters α , σ and the quark masses are fixed by fitting the zero temperature quarkonium spectrum as in [13, 14]. The parameters employed are given by $\alpha = 0.471$, $\sigma = 0.192 \text{ GeV}^{\nu+1}$, $m_c = 1.32 \text{ GeV}$ and $m_b = 4.746 \text{ GeV}$ by fitting the zero temperature quarkonia spectrum. The spin average masses and the wave functions are obtained by solving the schrodinger equation numerically using the screened potential of Eqn. 6 as quark-antiquark interaction potential at a given temperature.

In the relativistic quark model, the decay constant can be expressed through the meson wave function $\Phi_{P/V}(p)$

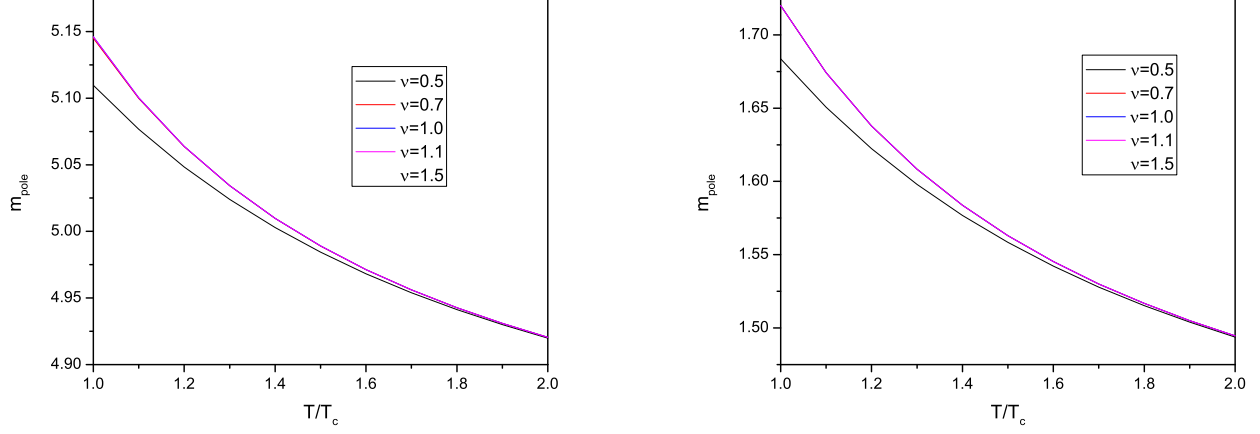


FIG. 2. The pole mass for bottom quark for screened coulomb potential at different potential exponent (a) for $b\bar{b}$ system (b) for $c\bar{c}$ system

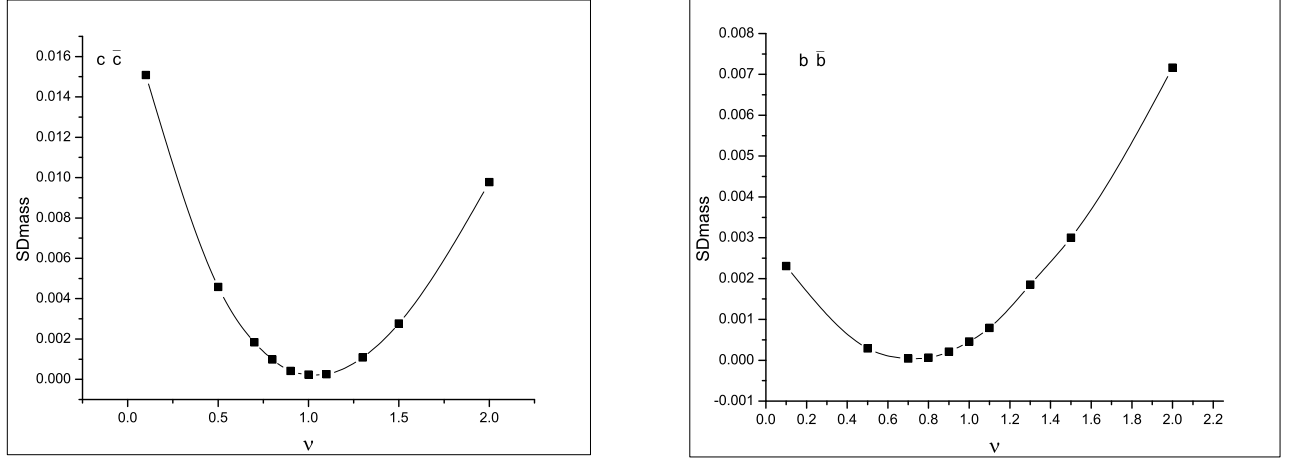


FIG. 3. rms deviation in zero temperature mass for quarkonia states taken from [13] (a) for charmonium states (b) for bottomonium states

in the momentum space [15],

$$f_{P/V} = \sqrt{\frac{12}{M_{P/V}}} \int \frac{d^3p}{(2\pi)^3} \sqrt{\left(\frac{E_Q(p) + m_Q}{2E_Q(p)}\right) \left(\frac{E_{\bar{Q}}(p) + m_{\bar{Q}}}{2E_{\bar{Q}}(p)}\right)} \left\{ 1 + \frac{\lambda_{P/V} p^2}{[E_Q(p) + m_Q][E_{\bar{Q}}(p) + m_{\bar{Q}}]} \right\} \Phi_{P/V}(p)$$

with $\lambda_P = -1$ and $\lambda_V = -1/3$. In the nonrelativistic limit $\frac{p^2}{m^2} \ll 1.0$, this expression reduces to the well known relation between $f_{P/V}$ and the ground state wave function at the origin $R_{P/V}(0)$ through the Van-Royen-Weisskopf formula [16]. Though most of the models predict the meson mass spectrum successfully, there exist wide range of predictions of their decay constants. For example, the ratio $\frac{f_P}{f_V}$ was predicted to be > 1

in most of the nonrelativistic cases, as $m_P < m_V$ and their wave function at the origin assumed to be the same $R_P(0) \sim R_V(0)$ [17]. The ratio computed in the relativistic models [18] have predicted $\frac{f_P}{f_V} < 1$, particularly in the $Q\bar{Q}$ sector, but $\frac{f_P}{f_V} > 1$ in the heavy-light flavour sector. This disparity on the predictions of the decay constants play decisive role in the decay properties of these mesons. The value of the radial wave function (R_P) for 0^{-+} and (R_V) for 1^{--} states would be different due to their spin dependent hyperfine interaction. The spin hyperfine interaction of the heavy flavour mesons are small and this can cause a small shift in the value of the wave function at the origin. Though, many models neglect this difference between (R_P) and (R_V), we consider this correction by making an ansatz that the $R_{P/V}(0)$ are related to the

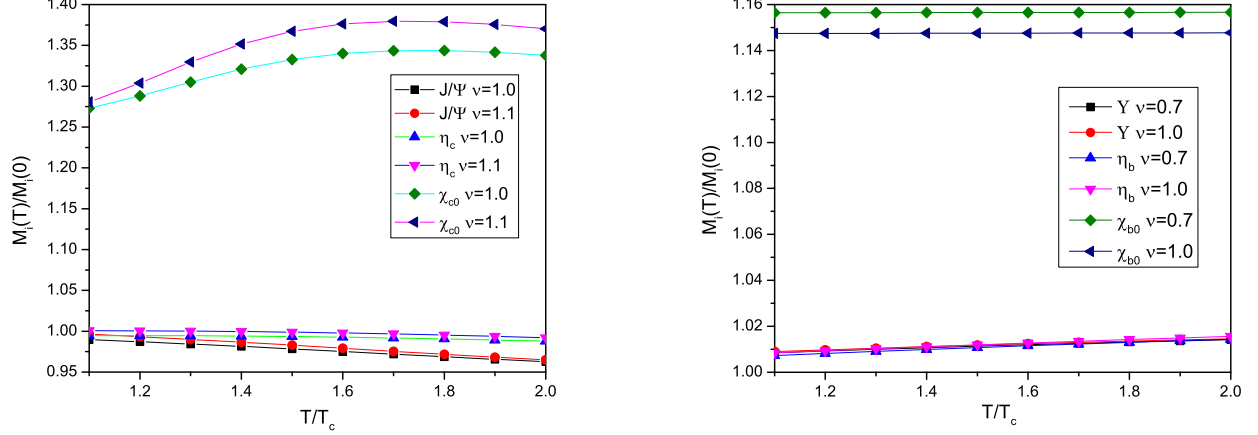


FIG. 4. Ratio of the mass at given temperature to the zero temperature mass for different quarkonium states at different potential exponent ν (a) for charmonium (b) for bottomonium.

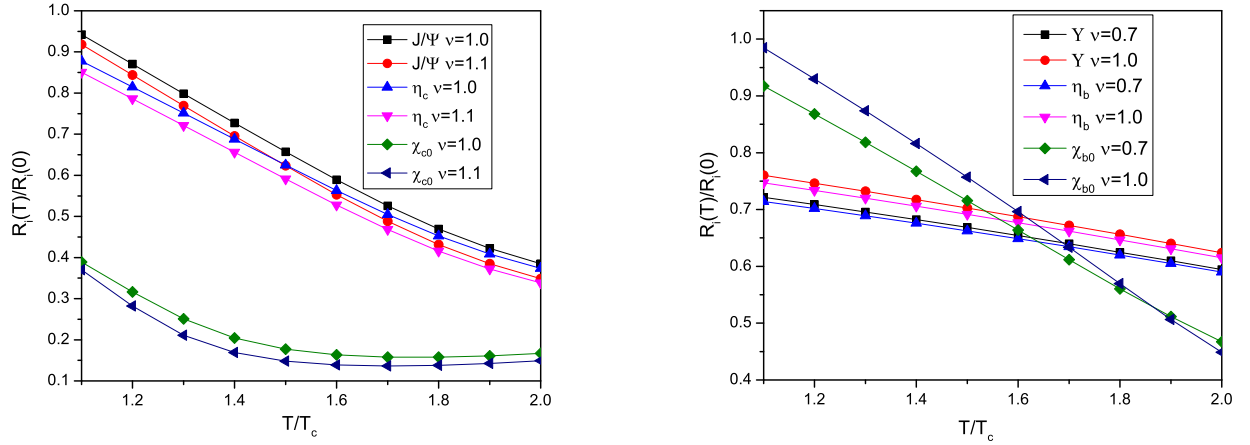


FIG. 5. Ratio of the wave function at zero separation at given temperature $R_i(T)$ to the zero temperature wave function $R_i(0)$ for different quarkonium states at different potential exponent ν (a) for charmonium (b) for bottomonium.

value of the radial wave function at the origin, $R_n(0)$ according to the same way their masses are related. Thus, by considering

$$M_{nP/V} = M_{n,CW} \left[1 + (SF)_{P/V} \frac{\langle V_{SS} \rangle_n}{M_{n,CW}} \right] \quad (9)$$

and following the fact that any c -number, a , commutes with the Hamiltonian, *i.e.* $aH\Psi = H(a\Psi)$, we express [19],

$$R_{nP/V}(0) = R_n(0) \left[1 + (SF)_{P/V} \frac{(M_{nV} - M_{nP})}{M_{n,CW}} \right] \quad (10)$$

Here $(SF)_P = -\frac{3}{4}$ and $(SF)_V = \frac{1}{4}$ are the spin factor corresponding to the pseudoscalar ($J = 0$) spin coupling

and vector ($J = 1$) spin coupling respectively. $M_{n,CW}$ and $R_n(0)$ are spin average mass and the normalized spin independent wave function at the origin of the meson state respectively. It can easily be seen that this expression given by Eqn 10 is consistent with the relation

$$R(0) = \frac{3R_V(0) + R_P(0)}{4} \quad (11)$$

given by [19, 20] for nS states. By incorporating first order QCD correction to the Van Royen-Weiskopff formula, the decay constant is computed as [21, 22],

$$f_{P/V}^2(nS) = \frac{3 \left| R_{nP/V}^{(\ell)}(0) \right|^2}{\pi M_{nP/V}} \bar{C}^2(\alpha_s) \quad (12)$$

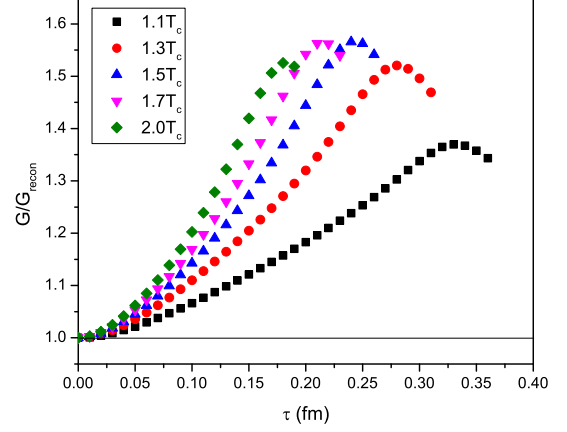
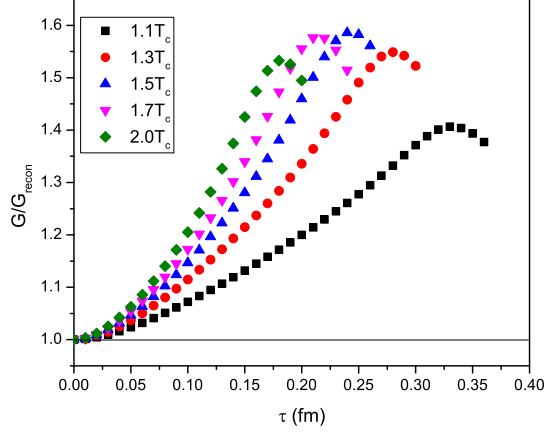


FIG. 6. G/G_{recon} for pseudoscalar charmonium (η_c) state (a) for $\nu = 1.0$ (b) for $\nu = 1.1$

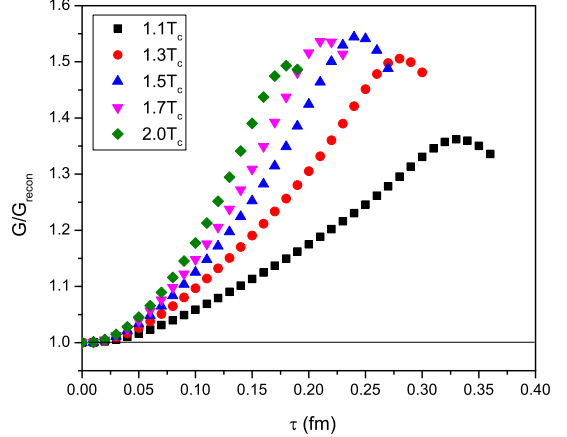
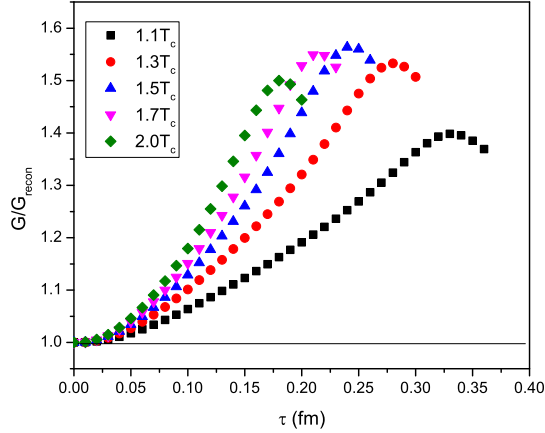


FIG. 7. G/G_{recon} for vector charmonium (J/ψ) state (a) for $\nu = 1.0$ (b) for $\nu = 1.1$

where, the first order QCD correction, $\bar{C}(\alpha_s)$ is expressed for the $Q\bar{Q}$ system as

$$\bar{C}(\alpha_s) = 1 - \frac{\alpha_s}{\pi} \delta^{V,P} \quad (13)$$

Here $\delta^V = \frac{8}{3}$ [21, 22] and $\delta^P = 2$ [21–23].

IV. TEMPERATURE AND THE EXPONENT (ν) DEPENDANCE ON THE CORRELATORS

The temperature dependant energy eigen values (E_i) and the wave functions are obtained by solving the schrodinger equation numerically [24]. The spin average mass (M_{sa}) is given by $M_{sa} = 2m_i + E_i$. Once M_{sa} is obtained, then the mass of the quarkonia state is computed using Eqn. 9. For computing the mass difference

between different spin degenerate mesonic states, we consider the spin dependent part of the usual one gluon exchange potential (OGEP) given by [25–29]. Accordingly, the spin-dependent part, $V_{SD}(r)$ contains three types of interaction terms, such as the spin-spin, the spin-orbit and the tensor part as

$$V_{SD}(r) = V_{SS}(r) \left[S(S+1) - \frac{3}{2} \right] + V_{LS}(r) (\vec{L} \cdot \vec{S}) + V_T(r) \left[S(S+1) - \frac{3(\vec{S} \cdot \vec{r})(\vec{S} \cdot \vec{r})}{r^2} \right] \quad (14)$$

The spin-orbit term containing $V_{LS}(r)$ and the tensor term containing $V_T(r)$ describe the fine structure of the meson states, while the spin-spin term containing $V_{SS}(r)$ proportional to $2(\vec{s}_q \cdot \vec{s}_{\bar{q}}) = S(S+1) - \frac{3}{2}$ gives the spin singlet-triplet hyperfine splitting. The coefficient of these

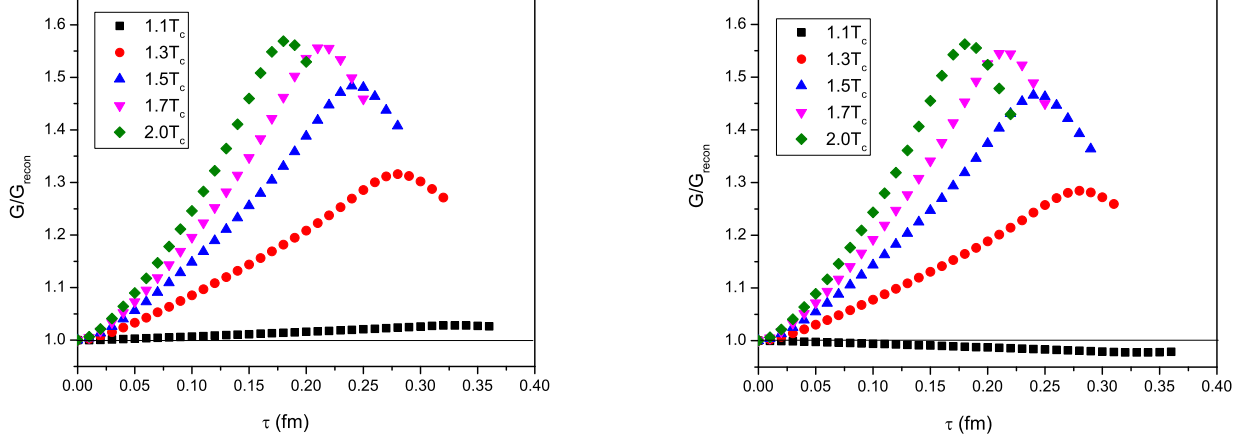


FIG. 8. G/G_{recon} for scalar charmonium state (χ_{c0}) (a) for $\nu = 1.0$ (b) for $\nu = 1.1$

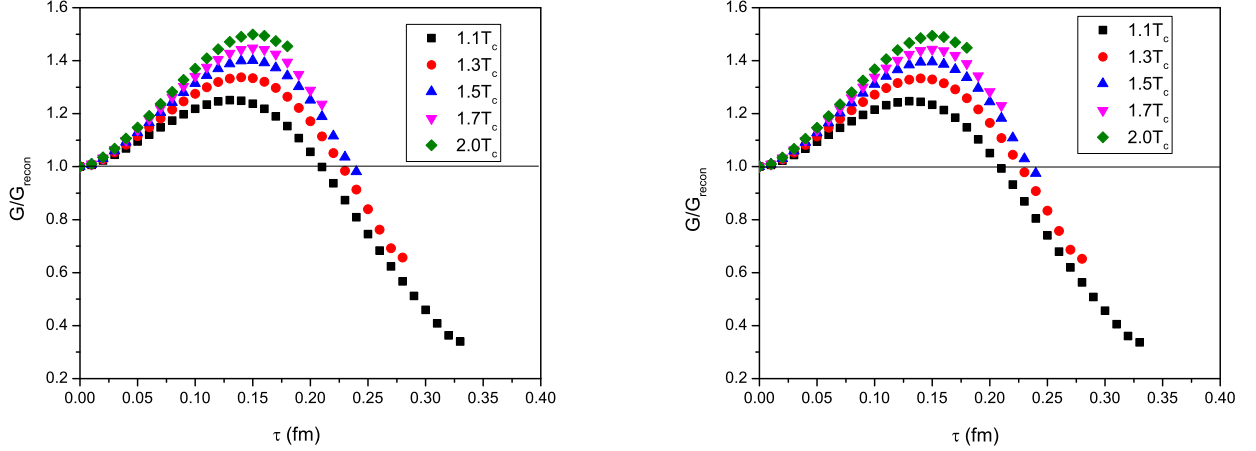


FIG. 9. G/G_{recon} for pseudoscalar bottomonium state (η_b) (a) for $\nu = 0.7$ (b) for $\nu = 1.0$

TABLE II. Spin averaged mass (M_{sa}) in GeV for charmonium and bottomonium states for different choices of potential exponent ν

T/T_c	Charmonium state								Bottomonium state							
	1S				1P				1S				1P			
	$\nu=0.5$	1.0	1.1	1.5	0.5	1.0	1.1	1.5	0.5	0.7	1.0	1.5	0.5	0.7	1.0	1.5
1.1	2.930	3.040	3.060	3.129	3.063	3.274	3.306	3.370	9.515	9.519	9.525	9.535	9.787	9.831	9.891	9.976
1.2	2.929	3.034	3.053	3.115	3.053	3.242	3.268	3.305	9.523	9.527	9.533	9.542	9.787	9.829	9.887	9.967
1.3	2.928	3.028	3.045	3.100	3.042	3.211	3.229	3.254	9.530	9.534	9.540	9.549	9.786	9.827	9.883	9.958
1.4	2.926	3.021	3.036	3.085	3.033	3.181	3.195	3.212	9.537	9.541	9.547	9.555	9.784	9.824	9.878	9.947
1.5	2.923	3.013	3.027	3.070	3.024	3.154	3.165	3.179	9.544	9.548	9.554	9.562	9.782	9.821	9.872	9.935
1.6	2.921	3.005	3.018	3.054	3.018	3.132	3.141	3.153	9.550	9.554	9.560	9.568	9.780	9.817	9.865	9.922
1.7	2.918	2.997	3.008	3.039	3.013	3.113	3.121	3.131	9.556	9.560	9.566	9.573	9.776	9.813	9.858	9.907
1.8	2.915	2.989	2.999	3.025	3.009	3.099	3.105	3.114	9.562	9.566	9.572	9.579	9.773	9.808	9.850	9.892
1.9	2.912	2.980	2.989	3.012	3.007	3.087	3.093	3.101	9.568	9.572	9.577	9.584	9.769	9.803	9.842	9.876
2.0	2.910	2.973	2.981	3.000	3.007	3.079	3.084	3.091	9.573	9.577	9.582	9.589	9.766	9.797	9.834	9.862

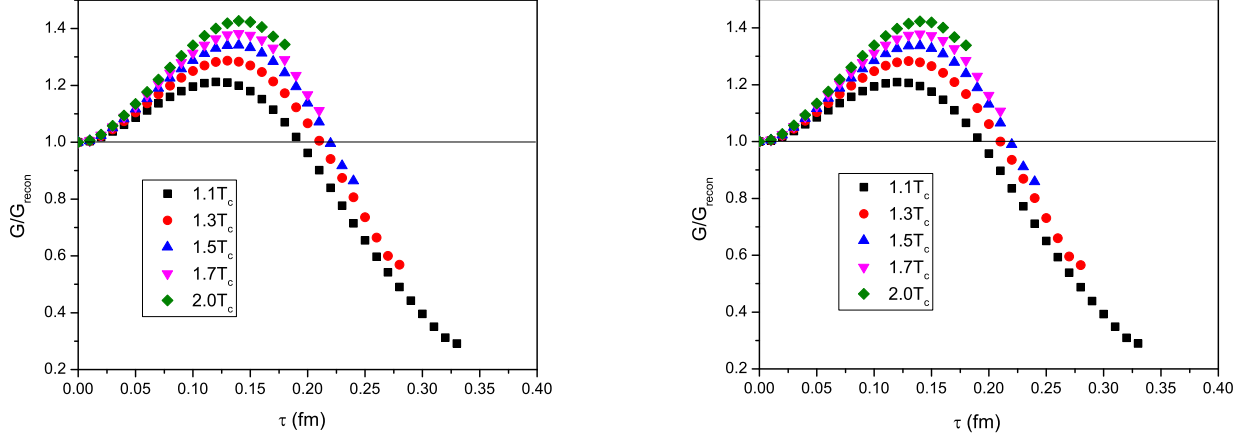


FIG. 10. G/G_{recon} for vector bottomonium state (Υ) $\nu = 0.7$ (a) for $\nu = 0.7$ (b) for $\nu = 1.0$

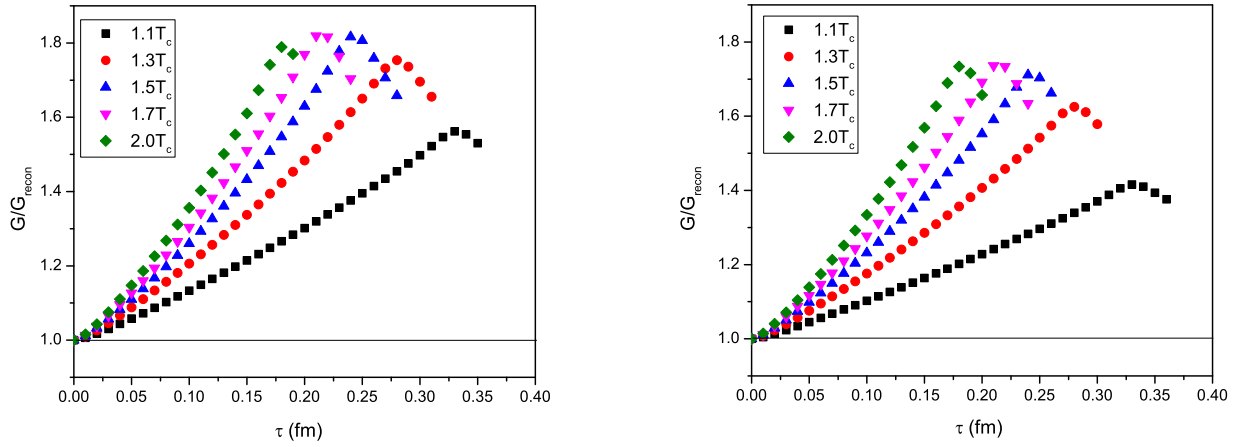


FIG. 11. G/G_{recon} for scalar bottomonium state (χ_{b0}) (a) for $\nu = 0.7$ (b) for $\nu = 1.0$

TABLE III. Masses of charmonium states in GeV for different choices of potential exponent ν

T/T_c	η_c				J/ψ				χ_{c0}			
	$\nu=0.5$	1.0	1.1	1.5	0.5	1.0	1.1	1.5	0.5	1.0	1.1	1.5
1.1	2.886	2.960	2.973	3.020	2.945	3.067	3.089	3.166	4.312	4.412	4.469	5.482
1.2	2.888	2.960	2.973	3.017	2.943	3.059	3.079	3.148	4.323	4.464	4.549	5.930
1.3	2.889	2.959	2.972	3.014	2.940	3.051	3.069	3.129	4.332	4.523	4.639	6.197
1.4	2.890	2.958	2.970	3.010	2.938	3.041	3.058	3.110	4.337	4.578	4.716	6.322
1.5	2.890	2.957	2.968	3.006	2.934	3.032	3.047	3.091	4.337	4.619	4.770	6.350
1.6	2.890	2.955	2.965	3.000	2.931	3.022	3.035	3.072	4.334	4.645	4.801	6.318
1.7	2.890	2.952	2.962	2.993	2.927	3.012	3.024	3.054	4.327	4.656	4.814	6.249
1.8	2.889	2.948	2.957	2.985	2.924	3.002	3.012	3.038	4.319	4.657	4.812	6.160
1.9	2.887	2.944	2.952	2.977	2.921	2.993	3.002	3.023	4.309	4.650	4.800	6.059
2.0	2.886	2.940	2.947	2.969	2.918	2.984	2.992	3.010	4.297	4.637	4.781	5.955

TABLE IV. Masses of bottomonium states in GeV for different choices of potential exponent ν

T/T_c	η_b				Υ				χ_{b0}			
	$\nu=0.5$	0.7	1.0	1.5	0.5	0.7	1.0	1.5	0.5	0.7	1.0	1.5
1.1	9.464	9.464	9.464	9.465	9.532	9.538	9.546	9.558	11.359	11.359	11.360	11.361
1.2	9.472	9.472	9.472	9.474	9.540	9.545	9.553	9.565	11.359	11.359	11.360	11.361
1.3	9.481	9.480	9.481	9.482	9.547	9.552	9.560	9.571	11.359	11.359	11.360	11.361
1.4	9.489	9.488	9.489	9.490	9.554	9.559	9.567	9.577	11.359	11.360	11.360	11.362
1.5	9.496	9.496	9.497	9.498	9.560	9.565	9.573	9.583	11.360	11.360	11.360	11.363
1.6	9.504	9.504	9.504	9.505	9.566	9.571	9.579	9.589	11.360	11.360	11.361	11.363
1.7	9.511	9.511	9.511	9.512	9.572	9.577	9.584	9.594	11.360	11.360	11.361	11.365
1.8	9.517	9.518	9.518	9.519	9.577	9.582	9.589	9.599	11.360	11.360	11.361	11.366
1.9	9.524	9.524	9.525	9.526	9.582	9.587	9.594	9.603	11.360	11.361	11.362	11.367
2.0	9.530	9.531	9.531	9.532	9.587	9.592	9.599	9.608	11.360	11.361	11.362	11.369

TABLE V. ℓ^{th} derivative of radial wave function at zero separation for charmonium states in $GeV^{\ell+3/2}$ for different choices of potential exponent ν

T/T_c	η_c				J/ψ				χ_{c0}			
	$\nu=0.5$	1.0	1.1	1.5	0.5	1.0	1.1	1.5	0.5	1.0	1.1	1.5
1.1	0.239	0.423	0.456	0.565	0.249	0.454	0.492	0.620	0.051	0.102	0.106	0.047
1.2	0.224	0.392	0.421	0.509	0.232	0.419	0.452	0.554	0.046	0.083	0.080	0.033
1.3	0.208	0.362	0.387	0.453	0.216	0.385	0.412	0.488	0.042	0.066	0.060	0.029
1.4	0.193	0.331	0.352	0.396	0.200	0.350	0.373	0.423	0.039	0.054	0.048	0.028
1.5	0.179	0.301	0.317	0.341	0.184	0.317	0.334	0.361	0.037	0.047	0.042	0.028
1.6	0.165	0.271	0.283	0.290	0.170	0.284	0.296	0.304	0.037	0.043	0.040	0.029
1.7	0.154	0.243	0.251	0.247	0.158	0.253	0.262	0.257	0.037	0.042	0.039	0.030
1.8	0.144	0.218	0.223	0.212	0.147	0.226	0.231	0.220	0.038	0.041	0.039	0.032
1.9	0.136	0.197	0.200	0.187	0.139	0.203	0.206	0.193	0.040	0.042	0.041	0.035
2.0	0.130	0.180	0.181	0.169	0.133	0.185	0.187	0.174	0.042	0.044	0.042	0.038

spin-dependent terms of Eqn.14 can be written in terms of the vector (V_V) or coulomb part and scalar (V_S) or confinement part of the static potential, $V(r)$ described in Eqn. 6 as [27]

$$V_{LS}(r) = \frac{1}{2 m_1 m_2 r} \left(3 \frac{dV_V}{dr} - \frac{dV_S}{dr} \right) \quad (15)$$

$$V_T(r) = \frac{1}{6 m_1 m_2} \left(3 \frac{d^2 V_V}{dr^2} - \frac{1}{r} \frac{dV_V}{dr} \right) \quad (16)$$

$$V_{SS}(r) = \frac{16 \pi \alpha_s}{9 m_1 m_2} \delta^{(3)}(\vec{r}) \quad (17)$$

The spin average masses (M_{sa}) for both charmonium and bottomonium states are tabulated in Table II. The quarkonia masses for both charmonium and bottomonium states are shown in Table III and IV respectively. Similarly the ℓ^{th} derivative of the radial wave function at zero separation for charmonium and bottomonium states are shown in Table V and VI respectively. The choices of the potential exponent $\nu = 1.1$ for charmonium state and

$\nu = 0.7$ for bottomonium state correspond to the minimum of the standard deviation in the mass (SD_{min}) in zero temperature potential as observed in our previous study [13] as shown in Fig. 3. The temperature dependant masses of the quarkonia states in terms of their zero temperature masses ($M_i(T)/M_i(0)$) are computed for $T > T_c$ and for different choices of the potential exponent, ν are shown in Fig. 4, similarly the ratio for the wavefunction is shown in Fig. 5. The ratio in mass for the P-state is found to be larger compare to the S-state quarkonia states. The ratio in the wave function decreases with increasing temperature for all quarkonium states. Finally, the decay constants are computed with help of Eqn. 12.

Our computed Spin average masses (M_{sa}) and the decay constants ($f_{p/v}$) corresponding to the choices of $\nu = 1.1$ in the charmonia and $\nu = 0.7$ in the case of bottomonia are then employed to predict the spectral functions given in Eqn. 3. We have also computed spectral function for the choices $\nu = 1.0$ in both the cases for the purpose of comparison with cornel like interactions considered by others [3, 30]. Further the euclidean correlators are computed using Eqn. 1. The present ratio G/G_{recon} are

TABLE VI. ℓ^{th} derivative of radial wave function at zero separation for bottomonium states in $GeV^{\ell+3/2}$ for different choices of potential exponent ν

T/T_c	η_b				Υ				χ_{b0}			
	$\nu=0.5$	0.7	1.0	1.5	0.5	0.7	1.0	1.5	0.5	0.7	1.0	1.5
1.1	6.810	7.385	8.147	9.182	6.909	7.502	8.289	9.363	0.527	0.671	0.874	1.168
1.2	6.695	7.258	8.001	9.005	6.791	7.370	8.138	9.179	0.498	0.635	0.826	1.089
1.3	6.575	7.125	7.852	8.826	6.668	7.234	7.983	8.993	0.468	0.598	0.776	1.006
1.4	6.451	6.990	7.698	8.642	6.540	7.095	7.825	8.802	0.437	0.561	0.725	0.917
1.5	6.322	6.851	7.542	8.455	6.407	6.951	7.663	8.608	0.407	0.524	0.672	0.822
1.6	6.189	6.707	7.381	8.266	6.271	6.803	7.497	8.412	0.376	0.485	0.618	0.715
1.7	6.054	6.560	7.217	8.072	6.132	6.652	7.328	8.211	0.347	0.447	0.563	0.597
1.8	5.915	6.409	7.051	7.876	5.989	6.497	7.157	8.008	0.319	0.410	0.506	0.483
1.9	5.771	6.257	6.881	7.676	5.841	6.340	6.981	7.802	0.294	0.374	0.450	0.392
2.0	5.626	6.100	6.707	7.475	5.693	6.179	6.803	7.594	0.273	0.342	0.398	0.331

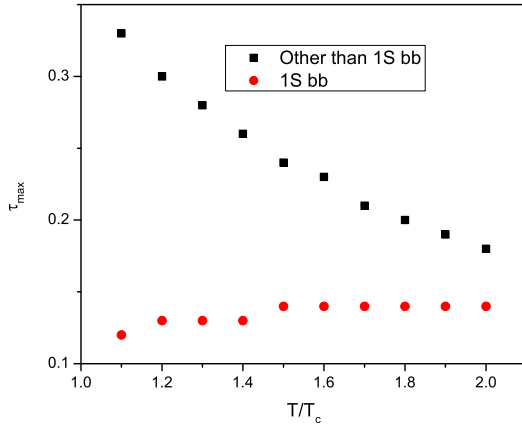


FIG. 12. τ_{max} vs. T/T_c for all quarkonia states

drawn in Figs. 6, 7, 8, 9, 10 and 11 for the euclidean time τ in between $\tau = 0$ to $\tau = 1/T$. The plots of these figures correspond to different choice of $T/T_c \leq 2.0$.

V. RESULTS AND DISCUSSION

As from Fig. 4 $M_i(T)/M_i(0)$ for J/ψ and η_c case found to decrease continuously with T/T_c for all the range of T/T_c . The behaviour is same for both the choices of $\nu = 1.0$ and $\nu = 1.1$ except the magnitude of $M_i(T)/M_i(0)$ increases slightly with ν . While $M_i(T)/M_i(0)$ for χ_{c0} found to increase upto $T/T_c = 1.7$ then, start slightly decreasing. However, in the case of $b\bar{b}$ system $M_i(T)/M_i(0)$ for all η_b , Υ and χ_{b0} states found to increases with T/T_c for all T in the range of $T/T_c \leq 2.0$. So, the medium effect in the η_c and J/ψ are opposite to that of η_b and Υ states.

From, Fig. 5 $R_i(T)/R_i(0)$ for η_c and J/ψ states found

to decrease monotonically with increase in T/T_c , while $R_i^{(\ell)}(T)/R_i^{(\ell)}(0)$ for χ_{c0} state found to decrease upto $T/T_c = 1.7$ then it is increasing slightly. $R_i(T)/R_i(0)$ for η_b and Υ states found to decrease monotonically for all the range of T/T_c . $R_i^{(\ell)}(T)/R_i^{(\ell)}(0)$ for χ_{b0} state also found to decrease much faster than η_b and Υ states. These observations are same for both $\nu = 1.0$ and $\nu = 0.7$ except their magnitudes are higher.

The correlators at the different T/T_c obtained are found to have a similar behaviour with increase in τ . In the case of charmonia state, correlators attain maxima at different values of τ and it shifts towards lower τ as T/T_c increases. While in the case of η_b and Υ bottomonia the maxima of the correlators are found to shift slightly towards higher τ . Whereas, the behaviour in the case of χ_{b0} belongs to that of charmonia states. To make this observation more clear we plot the values of τ at the maximum correlator (τ_{max}) against T/T_c in Fig. 12 for both the case of $b\bar{b}$ and $c\bar{c}$. It is very striking to see that values of τ at which G/G_{recon} is maximum (τ_{max}) is same for η_c , J/ψ , χ_{c0} and χ_{b0} states with a chosen T/T_c , and τ_{max} decreases with T/T_c . This behaviour is shown graphically in Fig. 12 Here we also shown the behaviour of τ_{max} vs T/T_c in the case of η_b and Υ system. It seems that both the curves leading towards a common saturated value beyond $T/T_c > 2.0$. Our results do not show any major deviation with the potential exponent ν . However, from Fig. 8 (b), we find G/G_{recon} at $T/T_c = 1.1$ of χ_{c0} decreases from 1.0 as τ increases while similar case in Fig. 8 (a) for $\nu = 1.0$ seems to increase from 1.0 as τ increases. From Fig. 10 and Fig. 9 we also notice that G/G_{recon} in η_b and Υ decreases below 1.0 relatively at lower τ values compared to all other states studied here. The τ dependance of the correlators are found to be sensitive to the choices of the continuum threshold s_0 .

As seen from Fig. 6 our obtained G/G_{recon} shows agreement with the early potential model [3] but differs from the lattice results [6] where G/G_{recon} remains to unity upto $\tau \approx 0.05 fm$ then it starts gradually falling. Our results shows same trend to QCD sum rule results [30] at

$T = 1.1T_c$.

Fig. 7 represents G/G_{recon} for vector charmonium states (J/ψ). For smaller values of τ our results agrees with the lattice [6] and also with the QCD sum rules [30]. Though the present G/G_{recon} in the case of η_c increases from 1.0, the results based on fine isotropic lattice study shows decreases from 1.0 for all temperatures. However the general behaviour of all other states are in accordance with the lattice results [4, 6]. As, the η_c and J/ψ corresponds to same 1S state, one do not expect their correlators to behave differently.

Fig. 8 represents G/G_{recon} for scalar channel of 1P charmonium state (χ_{c0}). Here, also our results agrees with lattice [6] and QCD sum rules [30].

Similarly, Figs. 9, 10 and 11 represent our results for 1S pseudoscalar (η_b), 1S vector (Υ) and 1P scalar (χ_{b0}) bottomonium states respectively. Our results agrees with earlier potential model [3] but contradicts with lattice results [5]. The lattice results for η_b case shows unity behaviour for temperature upto $2.30T_c$. The weaker dependance of the correlators on temperature was assumed as the melting of the states, but melting of state cannot be extracted from the correlators [32]. Similar to the charmonium case, our results for η_b and Υ shows the same behaviour as expected (because they belong to same 1S state of bottomonium system).

Variation in G/G_{recon} from unity represents dissolution of the quarkonium states into medium at higher temperature above T_c . Though, the lattice results for bottomonium states need to reexamined as the cutoff energy remains below the energy relevant to bottomonium systems [3].

τ for maximum occurrence of G/G_{recon} , τ_{max} represents the temperature for the maximum correlation of the quarkonia states. In our study, τ_{max} found to be exponentially decreasing with the temperature in the case of quarkonia states (except for $b\bar{b}(1S)$ case).

The values of G/G_{recon} below 1 corresponds to value of G to be lower than G_{recon} . This means the survival probability of the state to be lower than in the zero mode case or dissociation of the quarkonium state. Considering the time for $G/G_{recon} = 1$ related with the temperature T as, $\tau = 1/T$ we predict the dissociation temperature of η_c , J/ψ and χ_{c0} to be around $1.2T_c$ while η_b and Υ states can survive upto $3.0T_c$.

ACKNOWLEDGEMENT

Part of this work is carried out under the UGC grant with ref no. F.40-457/2011(SR). Arpit Parmar thanks UGC, India for the financial support under RFSMS scheme for the present work.

-
- [1] Gert Aarts *et al.*, Phys. Rev. D **76** 094513 (2007).
 - [2] R. Rappa, D. Blaschke and P. Crochet, Prog. Part. and Nucl. Phys. **65** 209 (2010).
 - [3] Agnes Mocsy and Peter Petreczky, Phys. Rev. D **73** 074007 (2006).
 - [4] Soumen Datta, Frithjof Karsch, Peter Petreczky and Ines Wetzorke, Phys. Rev. D **69** 094507 (2004).
 - [5] K. Petrov, A. Jakovac, P. Petreczky and A. Velytsky, Proc. Sci. LAT2005 153 (2005); arXiv:hep-lat/0509138.
 - [6] H.-T. Ding *et al.*, Phys. Rev. D **86** 014509 (2012).
 - [7] T Matsui and H Satz, Phys. Lett. B **178** 416 (1986).
 - [8] S. Digal, P. Petreczky and H. Satz, Phys. Rev. D **64** 094015 (2001).
 - [9] Agnes Mocsy and Peter Petreczky, J Phys. G **32** S515 (2006).
 - [10] E V Shuryak, Rev. Mod. Phys. **65** 1 (1993).
 - [11] F. Karsch, M.G. Mustafa and M.H. Thoma, Phys. Lett. B **497** 249 (2001).
 - [12] P Petreczky *et al.* Nucl. Phys. B: Proc. Suppl. **106** 513 (2002).
 - [13] Arpit Parmar, Bhavin Patel and P C Vinodkumar, Nucl. Phys. A **848** 299 (2010).
 - [14] S Jacobs, M G Olsson and C I Suchyta, Phys. Rev. D **33** 3338 (1986); **34** 3536 (E) (1986).
 - [15] Ebert D, Faustov R N and Galkin V O, Phys. Rev. **D67**, 014027 (2003).
 - [16] Van Royen R and Weisskopf V F, Nuovo Cimento **50**, (1967).
 - [17] Hwang D S and Gwang-Hee Kim, Z. Phys. **C76**, 107 (1997).
 - [18] Wang G L, Phys. Lett. **B633**, 492 (2006).
 - [19] Ajay Kumar Rai *et al.*, Phys. Rev. C **78** 055202 (2008).
 - [20] Bodwin G T, Lee J and Sinclair D K, Phys. Rev. **D51**, 1125 (1995).
 - [21] Berezhnoy A V, Kiselev V V and Likhoded A K, Z. Physik **A336**, 89 (1996).
 - [22] Braaten E and Fleming S, Phys. Rev. **D52**, 181 (1995).
 - [23] Gerstein S S *et al.*, arXiv:hep-ph/9803433v1.
 - [24] W Lucha and F Schoberl, Int. J. Mod. Phys. C **10** (1999) 607, arXiv:hep-ph/9811453.
 - [25] Branes T, Godfrey S and Swanson E S, Phys.Rev. **D72** (2005) 054026.
 - [26] Lakhina Olga and Swanson Eric S, Phys. Rev **D 74** (2006) 014012 [arXiv:hep-ph/0603164].
 - [27] Voloshin M B, Prog. Part. Nucl. Phys. **61** (2008) 455 arXiv:hep-ph/0711.4556.
 - [28] Eichten E, Godfrey S, Mahlke H and Rosner J L, Rev. Mod. Phys. **80** (2008) 1161.
 - [29] Gershtein S S, Kiselev V V, Likhoded A K and Tkabladze A V, Phys. Rev. **D51** (1995) 3613.
 - [30] Kenji Morita and Su Houn Lee, Phys. Rev. D **82** 054008.
 - [31] A. Jakovc *et al.*, Phys. Rev. D **75** 014506 (2007).
 - [32] N. Brambilla *et al.*, Eur. Phys. J C **71** 1534 (2011).